

Realization of multiscroll chaotic attractors by using current-feedback operational amplifiers

R. Trejo-Guerra and E. Tlelo-Cuautle

INAOE, Electronics Department,

Luis Enrique Erro 1, Tonantzintla, Puebla, 72840 México.

C. Sánchez-López

UAT, Department of Electronics Engineering,

Calzada Apizaquito, Apizaco, Tlaxcala, 90300 México.

J.M. Muñoz-Pacheco

UPP, Electronics and Telecommunications Department,

Puebla, 72640 México.

C. Cruz-Hernández

CICESE, Electronics and Telecommunications Department,

Km. 107, Carretera Tijuana-Ensenada, 22860 Ensenada, B.C., México.

Recibido el 8 de marzo de 2010; aceptado el 21 de mayo de 2010

Multiscroll chaotic attractors are physically implemented by using commercially available current-feedback operational amplifiers (CFOAs). The values of the circuit elements are obtained systematically by a proposed technique based in the saturation of the CFOA to create Piece-Wise Linear (PWL) functions. Herein the technique is verified by Spice simulations and in experimental form by using CFOAs to generate n -scroll attractors in a systematic way. Lyapunov exponents are given to prove the chaotic behavior.

Keywords: n -scroll attractors; Chua's circuit; break point; Lyapunov exponent; CFOA; PWL function.

Se realiza la implementación física de atractores caóticos de múltiples enrollamientos por medio del circuito comercial denominado amplificador operacional retroalimentado en corriente (CFOA). Los valores de los elementos del circuito son obtenidos sistemáticamente por medio de una técnica propuesta basada en la saturación del CFOA para generar funciones lineales a tramos (PWL functions). En este punto, la técnica es verificada por medio de simulaciones en Spice, así como de manera experimental utilizando CFOAs para generar atractores de n -enrollamientos de forma sistemática. Se presentan los exponentes de Lyapunov para corroborar el comportamiento caótico.

Descriptores: Atractores n -enrollamientos; circuito de Chua; punto de quiebre; exponente de Lyapunov; CFOA; función lineal a tramos.

PACS: 05.45.Pq; 05.45.Pq; 84.30.Ng; 07.50.Ek; 84.30.-r; 01.50.Pa

1. Introduction

Chaotic dynamical systems have been a subject of intensive research during several decades. Nowadays, it is used in describing particles motion [1], secure multimedia applications [2], parameter estimators [3], orbit stabilization [4], nonlinear function generators [5], and many others.

The generation of n -scroll attractors has been experimentally tested by Suykens et al. [6], who proposed a generalization for the Chua's circuit by adding more breakpoints to the nonlinear function; Yalçın *et al.* [7], developed a third order nonlinear system to generate chaotic scroll attractors in three directions usually called 3D attractors in spite of the form observed in the 3-state phase plane by using step functions; Lü *et al.* [8], presented similar results by using saturated functions, Han *et al.* [9,10], with the introduction of the hysteretic based multiscroll circuits, and Tang *et al.* [11], who proposed a technique for multiscroll circuits based on sinusoidal functions. In addition, some interesting applications have been introduced for these systems in the field of encryption, following a synchronization technique, for example Hamiltonian forms and observer approach [12]. Multiscroll oscilla-

tors provide more dynamical complexity than with traditional double-scroll oscillators.

The behavior of the nonlinear function has been generated by using hysteresis and piece-wise linear (PWL) functions such as: step function, saturated function or other interesting PWL approaches [13-15]. Simple circuits based on Opamps [8,10,16-19], operational transconductance amplifiers [8,20], current-feedback operational amplifiers (CFOAs) [7,21,22], Unity Gain Cells (UGCs) [23] and second generation current conveyors (CCII) [24,25], have been used in order to generate chaotic attractors. We remark that due to its simplicity, PWL approaches have demonstrated to be useful in the control of chaotic regime [26] and promising in nonlinear applications in dynamical system modeling [27].

Although chaos generators have been designed with Opamps, they have the drawback of working in low frequency due to the limitations on slew-rate and non-ideal phase of Opamps. To reach higher frequencies, other active devices should be considered. For instance, the CFOA has important advantages compared with conventional Opamps,

namely: wider bandwidth, high slew-rate and low power consumption [24, 25, 28].

On the other hand, while there have been reasonable advances in the construction of n-dimensional PWL functions [29, 30], the CMOS circuit implementation of these functions is subject of research. We remark the guidance given in Ref. 31, the function generator designed in Ref. 32 and the current mirror approach proposed in Ref. 33. In this paper a new CMOS-integrable nonlinear cell is introduced to generate CFOA-based PWL functions. Later, a parallel combination is proposed to increment the breakpoints in the PWL function. To customize such behavior, a simplified behavioral model is developed to compute the required circuit parameters. In order to show the usefulness of the proposed PWL function generation technique, we apply it to a known generalization of multiscroll Chua’s circuit. Lyapunov exponents are calculated for these systems to prove chaotic behavior.

Section 2 introduces the proposed saturation-based PWL generation technique with numerical results. Section 3 describes briefly the chaotic system and parameters for a generalization of the Chua’s circuit. Section 4 shows the computation of Lyapunov exponents that ensure chaotic behavior. Section 5 shows CFOA experimental implementations of multiscroll chaotic attractors. Finally, the conclusions are given in Sec. 6.

2. Saturation based PWL functions

The technique can be applied to produce in general, functions based in a set of contiguous arbitrary slopes m , each one delimited by a set of breakpoints $b_p < b_q$, where E is the middle point $E = b_p + Sat = b_q - Sat$ and $Sat = (b_q - b_p)/2$. In the following, we will restrict to symmetric PWL functions design, since this is the case of multiscroll chaotic systems generally described with canonical representations of PWL functions [34]. Figure 1a shows the proposed basic cell.

Basically, we assume that the saturated response of a CFOA amplifier can be linearized for all the range of the output signal which is beyond the last breakpoint of the respective PWL function. The circuit response is controlled by saturating the current follower of terminal Z; besides, a parallel connection results in a direct addition of signals. This makes the CFOA, a suitable circuit for the generation of PWL functions. The linearization approximation will depend on the circuit topology and technology [35]. However, Lyapunov exponents can be computed to probe chaotic behavior.

The CFOA has the following port relationships: $V_y = 0$, $V_x = A_v V_y$, $I_z = A_i I_x$ and $V_w = A_v V_z$. Where A_v and A_i are the voltage and current gains, respectively. In real applications, they are affected by the parasitic elements at each port. For instance, at X-port, R_x is the most dominant parasitic element [24]. It is around 50Ω for the commercial CFOA AD844. Routine analysis of Fig. 1a leads to (1). Where $R_X = R_{in} + R_x$ according with parasitics shown in Fig. 1b, the nonideal gains will be taken into account later.

First, we show how the saturated circuit works to produce PWL functions.

$$V_{out} = R_{out}(V_{in} - E)/R_X \tag{1}$$

By assuming that the signal in terminal Z is saturated when it reaches some threshold bias-dependent voltage V_{Zsat} , and if the output current remains constant (ideal case), then (1) is locally valid between boundaries

$$\begin{aligned} V^+ &= \frac{R_X}{R_{out}} V_{Zsat} + E, \\ V^- &= -\frac{R_X}{R_{out}} V_{Zsat} + E. \end{aligned} \tag{2}$$

The response of the proposed CFOA-based PWL cell shown in Fig. 1a, is described by:

$$V_{out}(V_{in}) = \begin{cases} \frac{R_{out}(V^- - E)}{R_X} & \text{if } V_{in} < V^-, \\ \frac{R_{out}(V_{in} - E)}{R_X} & \text{if } V^- < V_{in} < V^+, \\ \frac{R_{out}(V^+ - E)}{R_X} & \text{if } V_{in} > V^+. \end{cases} \tag{3}$$

If nonideal gains (A_v, A_i) and parasitics from Fig. 1b are taken into account, call $a_W = A_i^2 A_v$ the total gain at port W, and the ratios

$$\frac{R_z}{R_x + R_z} \quad \text{and} \quad \frac{R_z || R_{out}}{R_{out}}$$

at Z terminal of CFOA(a) and CFOA(b), respectively. However, for the saturated output Z, which is not able to follow the current signal, a linearized saturated output can be considered by the experimental value $a_{off} \approx 25 \times 10^{-3}$.

The nonlinear behavior of the proposed CFOA-based PWL cell can be described by

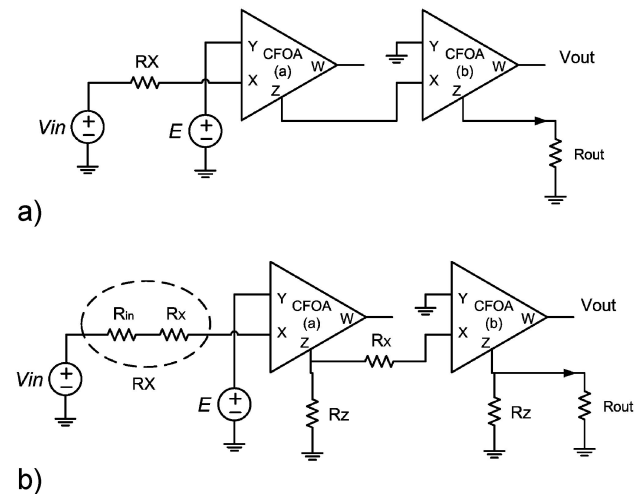


FIGURE 1. (a) New CFOA-based PWL cell, and (b) Circuit with parasitic resistances.

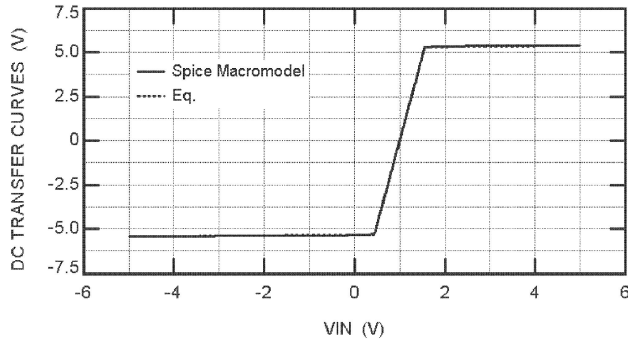


FIGURE 2. Comparison between Eq. (4) and the Spice macromodel with parameters $E = 1$, $R_X=5\text{ K}\Omega$ and $R_{out} = 50\text{ K}\Omega$.

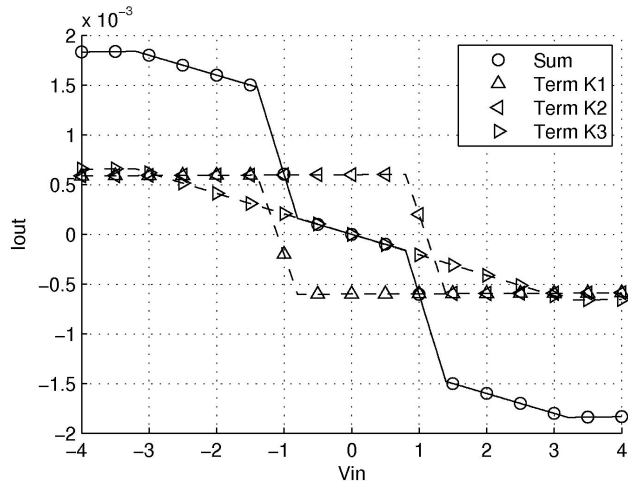


FIGURE 3. $v - i$ characteristic of Chua's diode to generate 3-scroll attractors showing each component.

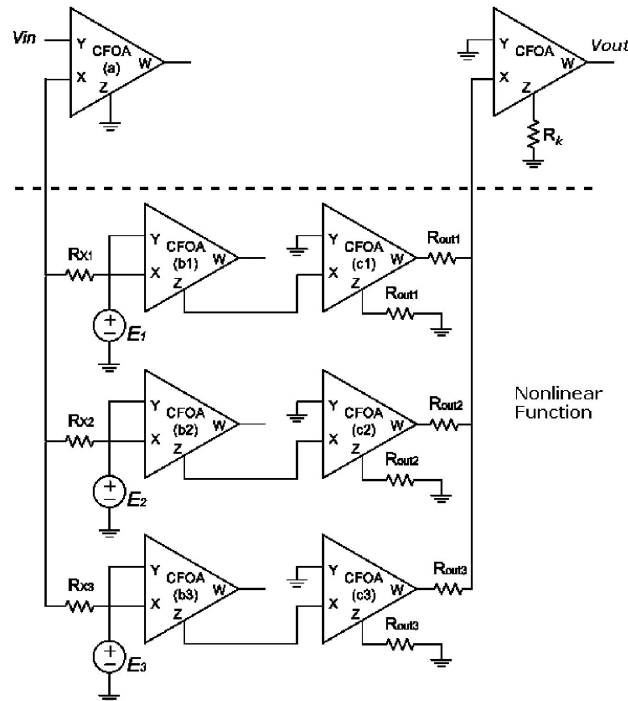


FIGURE 4. Parallel connection of nonlinear cells (Fig. 1) for a $v - v$ PWL-characteristic (Fig. 3) to generate 3-scroll attractor.

TABLE II. Circuit parameters.

E(V)	$R_X(\Omega)$	$R_{out}(\Omega)$
-1.1	4586	88458
1.1	4586	88458
0	44534	80536

$$K_1 = \frac{m_b - m_a}{c + j_1},$$

$$K_2 = \frac{m_b - m_a}{c + j_2},$$

$$K_3 = \frac{c^2(2m_a - m_b) + cm_a(j_2 + j_1) + m_b j_1 j_2}{(c + j_2)j_3(c + j_1)}. \quad (10)$$

As a result, the circuit of Fig. 4 is obtained with the parameters given in Table II for $V_{Zsat} = 5.3\text{ V}$ and a reduction of 14300 times for practical current levels. This is applied to a CFOA-based Chua's circuit to obtain a 3-scroll attractor.

3. Multiscroll Chua's circuit

We already mention in Sec. 1 the existence of diverse multiscroll systems. For convenience, we choose a generalization of the Chua's system described in Ref. 13; however, PWL functions can be applied to other multiscroll approaches. The dynamical system is described by (11) with parameters $\alpha = 10$, $\beta = 11.5$ and a nonlinear function given by (12), where $q = 1$ for $2n$ even scrolls, and $q = 2$ for $2n - 1$ odd scrolls. Vector m represents the slopes, while vector b shows the breakpoints. For an even number of scrolls m is taken as $[m_0..m_9]=[-4.416, -0.276, -3.036, -0.276, -3.036, -0.276, -3.036, -0.276, -3.036, -0.276]$ and $[b_1..b_9]=[0.1, 1.1, 1.55, 3.2, 3.85, 5.84, 6.6, 8.7, 9.45]$, while for an odd number of scrolls $[b_2..b_9]=[0.8, 1.4, 3.2, 3.9, 5.8, 6.4, 8.3, 9.2]$ is used.

$$\dot{x}_1 = \alpha(x_2 - x_1 - g(x_1)),$$

$$\dot{x}_2 = x_1 - x_2 + x_3,$$

$$\dot{x}_3 = -\beta x_2, \quad (11)$$

$$g(x_1) = m_{2n-1}x_1$$

$$+ \frac{1}{2} \sum_{i=q}^{2n-1} (m_{i-1} - m_i)(|x_1 + b_i| - |x_1 - b_i|). \quad (12)$$

4. Computing Lyapunov exponents

The Lyapunov exponents can be calculated from the state variables system description $\dot{x} = f(x)$ by applying several known methods [19, 36–38]. They are considered as indicators of chaotic behavior since they characterize the average divergence rates of small perturbations within the attractor

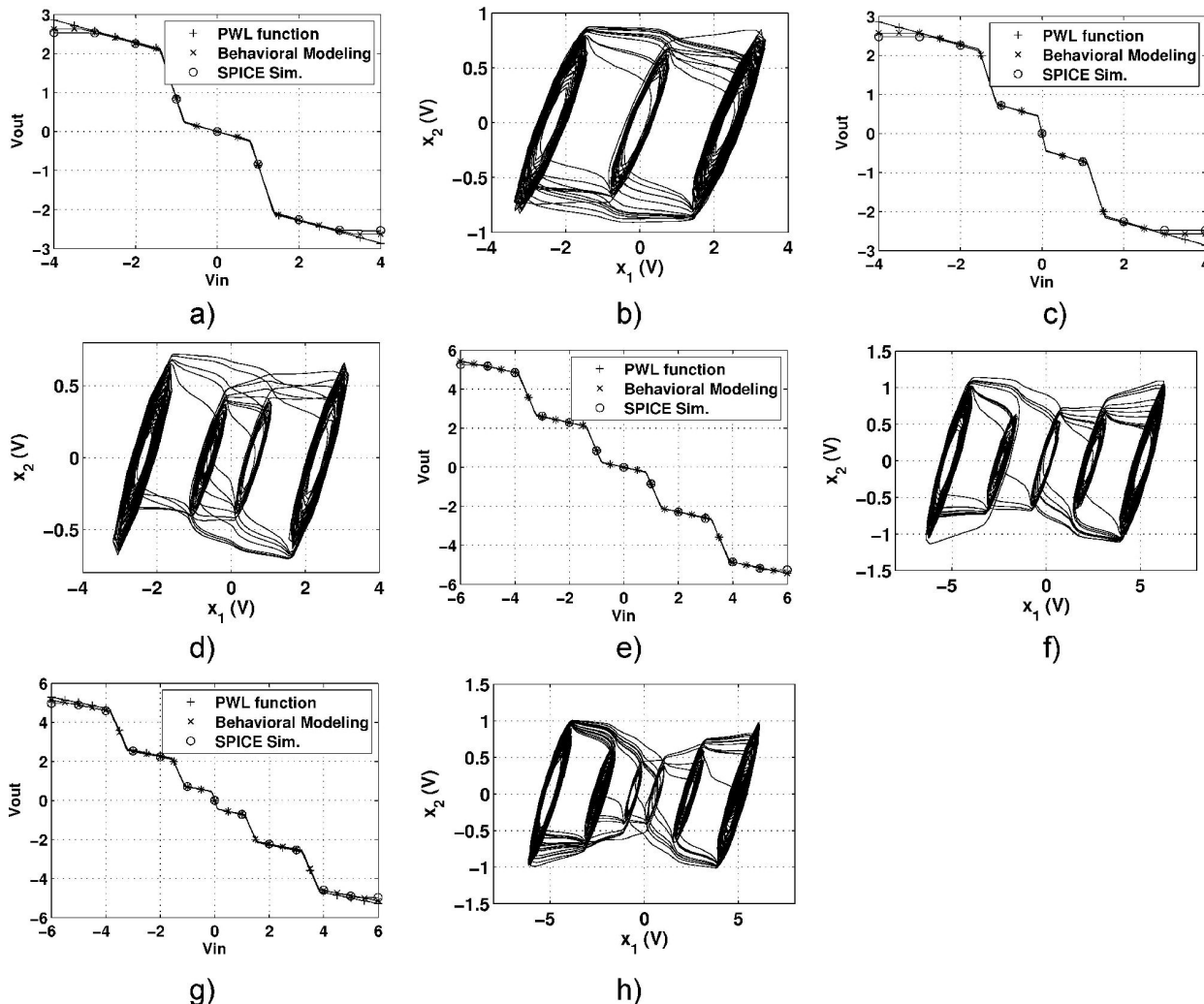


FIGURE 5. Spice simulations for 3, 4, 5, and 6-Scroll attractor. Nonlinearities comparisons are shown in: (a), (c), (e), and (g). Phase diagrams of the n -scroll attractor are shown in: (b), (d), (f), and (h).

TABLE III. Lyapunov exponents for each implementation ($\alpha = 10, \beta \approx 11.5$).

Attractor	λ_1	λ_2	λ_3
3-scroll	0.37958	0.00099	-7.7809
4-scroll	0.41808	0.00084	-7.6565
5-scroll	0.41051	0.00072	-7.7940
6-scroll	0.43760	0.00136	-7.5959

trajectories. A general method to calculate Lyapunov exponents in third order continuous dynamical systems is summarized as follows [39]:

- Initial conditions of the system are X_0 , for the variational system initial conditions are $I_{n \times n}$.
- Both systems are integrated until the orthonormalization period TO is reached. The integration of the variational system $Y = [y_1, y_2, y_3]$ is done by the current system X Jacobian in each step.

- The variational system Y is orthonormalized by using the standard Gram-Schmidt method [40], the natural logarithm of the norm of each Lyapunov vector is obtained and accumulated.
- Orthonormalized vectors are used as initial conditions of the next integration. This process is repeated until the full integration period T is completed.
- The Lyapunov exponents are obtained by:

$$\lambda_i \approx \frac{1}{T} \sum_{j=TO}^T \ln \| y_i \|$$

We chose a 0.00674 s integration time step and 0.71 s for the orthogonalization period TO ; initial conditions were $X_0 = [0.1, 0, 0]$ and a total integration steps of 500000. The Lyapunov exponents of the generalized Chua’s system are shown in Table III.

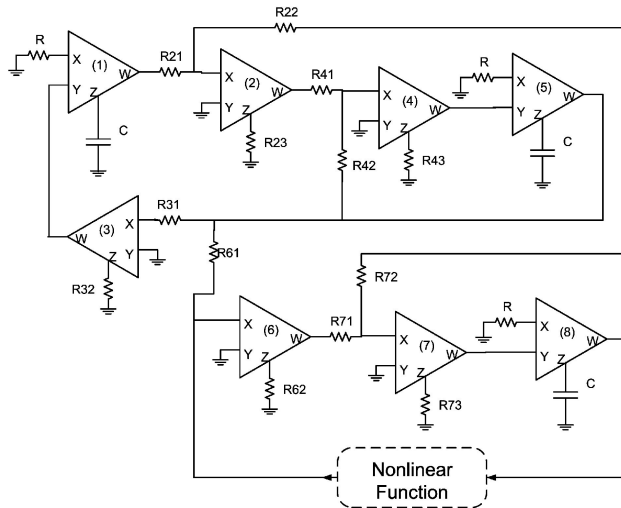


FIGURE 6. CFOA-based Chua's circuit.

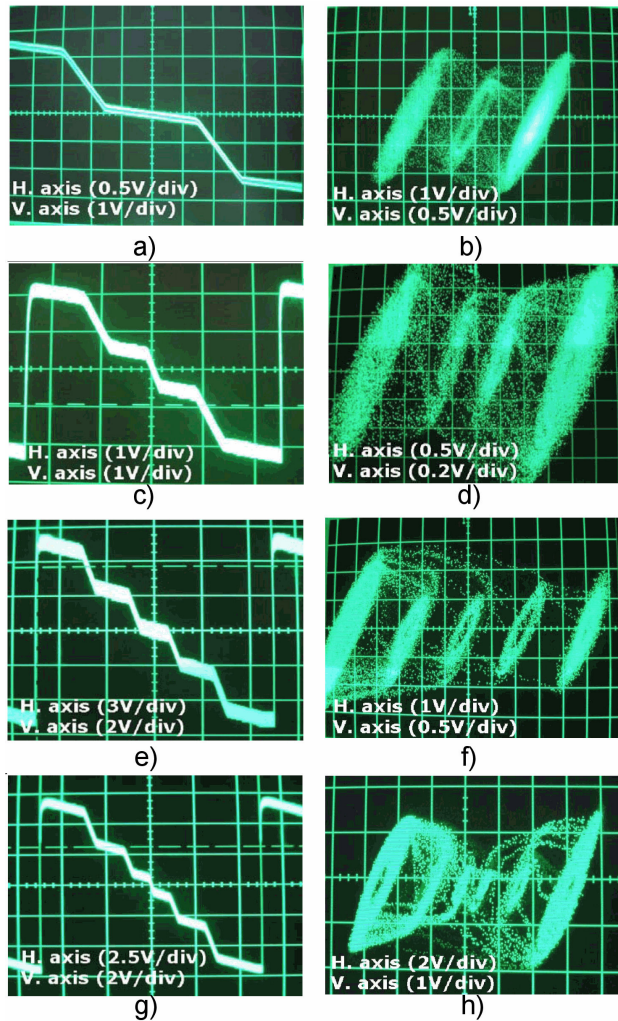


FIGURE 7. Experimental results for 3, 4, 5, and 6-scroll attractor. Nonlinearities are shown in: (a), (c), (e), and (g). Phase diagrams of the n -scroll attractor are shown in: (b), (d), (f), and (h). Horizontal axis is variable x_1 and vertical axis is x_2 . The dotted appearance is caused by the oscilloscope sampling.

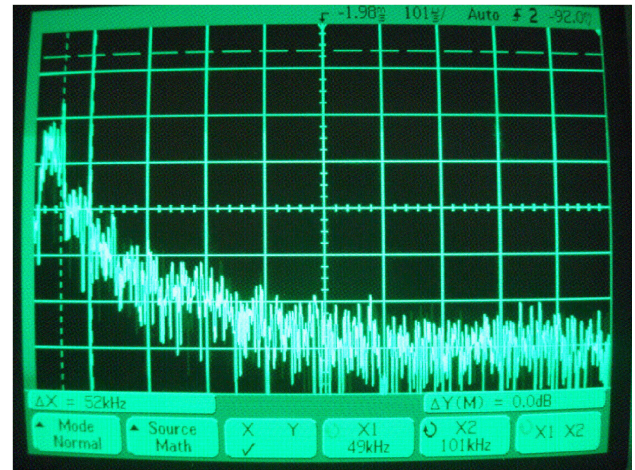


FIGURE 8. Frequency spectrum for the 6-scroll chaotic attractor showing 50 and 100 kHz peaks for state x_1 .

5. CFOA-based oscillators

The required PWL function (12) was observed to be identical to the proposed behavioral function (4) in the attractor region, thus allowing the generation of multi-scroll attractors by Spice simulation as shows Fig. 5. For experimental observations the chaotic oscillator was built directly by interconnecting integrator stages using CFOAs, see Fig. 6. An important issue for physical implementation is the characterization of the bias dependent parameter V_{Zsat} in spite of the different values shown by the simulation model and the real device.

5.1. Experimental observations

The developed PWL function was applied to the Chua's circuit of Fig. 6. Values of α and β correspond to coefficients $R_{73}/R_{72}=R_{73}/R_{71}$ and R_{32}/R_{31} , respectively. Resistances $R_{61} = R_{62}$ are set to properly adjust the PWL function gain, in the circuit. In this manner, the experiments show good agreement with theoretical and simulation results as shown in Fig. 7.

The frequency spectrum of state x_1 is observed for the 6-scroll attractor in Fig. 8, it shows two principal peaks; the first one is about 50 kHz while the second (corresponding to state x_2) is about 100 kHz.

6. Conclusion

A new circuit realization for multiscroll PWL based systems has been proposed by using saturated amplifiers. Basically, the $v - v$ PWL characteristic has been realized by using parallel connections of a proposed CFOA-based PWL cell. Using a generalization for the Chua's circuit, n -scroll attractors where obtained experimentally as shown in early works. To further prove the chaotic behavior of the system, a Lyapunov exponent's algorithm was reviewed and computed for some of the system implementations.

As a conclusion, a systematic approach is proposed to obtain the design parameters to realize symmetrical or non-symmetrical PWL functions. Most important is that the suitability of the proposed approach is demonstrated from experimental observations of the Chua's multiscroll circuit which are in good agreement with the theoretical analysis.

Acknowledgment

This work is supported by CONACyT-MEXICO through the scholarship 204229 and the project numbers 48396-Y,

J49593-Y, P50051, Promep UATLX-PTC-088 and by Consejería de Innovación, Ciencia y Empresa, Junta de Andalucía Spain, under the project TIC-2532. The second author acknowledge the CONACyT sabbatical leaves program for his stay at University of California at Riverside during 2009-2010. The third author thanks the support of the JAE-Doc program of CSIC, co-funded by FSE, Spain. We also acknowledges the participation of Roberto Toledo in the realization of the experiments.

1. R. Fossion and R. Bijker, *Rev. Mex. Fís.* **55** (2009) 41.
2. R. Hasimoto, *Rev. Mex. Fís.* **53** (2007) 332.
3. C. Aguilar-Ibanez, E. Hernandez-Rubio, and M.S. Suarez-Castanon, *Rev. Mex. Fís.* **53** (2007) 436.
4. C.A. Cruz-Villar, *Rev. Mex. Fís.* **53** (2007) 415.
5. E. Campos-Cantón, J.S. Murgía, I. Campos Cantón, and M. Chavira-Rodríguez, *Rev. Mex. Fís.* **53** (2007) 159.
6. J.A.K. Suykens, A. Huang, and L.O. Chua, *Int. J. Electron. Commun.* **51** (1997) 131.
7. M.E. Yalçın, J.A.K. Suykens, and J. Vandewalle, *Int. J. Bifurc. Chaos* **12** (2002) 23.
8. J. Lü, G. Chen, X. Yu, and H. Leung, *IEEE Trans. Circuits Syst. I* **51** (2004) 2476.
9. F. Han, J. Lü, X. Yu, and G. Chen, *Chaos Solitons Fractals* **28** (2006) 182.
10. F. Han, J. Lü, X. Yu, G. Chen, and Y. Feng, *Dynamics of Continuous Discrete and Impulsive Systems Series B* **12** (2005) 95.
11. K.S. Tang, G.Q. Zhong, G. Chen, and K.F. Man, *IEEE Trans. Circuits Syst. I* **48** (2001) 1369.
12. L. Gámez-Guzmán, C. Cruz-Hernández, R.M. López-Gutiérrez, and E.E. García-Guerrero, *Rev. Mex. Fís.* **54** (2008) 299.
13. G. Zhong, K.F. Man and G. Chen, *Int. J. Bifurc. Chaos* **12** (2002) 2907.
14. S. Yu, S. Qiu, and Q. Lin, *Sci in China F* **46** (2003) 14.
15. S. Yu, W.K.S. Tang, and G. Chen, *Int. J. Bifurc. Chaos* **17** (2007) 3951.
16. J.M. Muñoz-Pacheco and E. Tlelo-Cuautle, *J. App. Research Technol.* **7** (2009) 5.
17. R. Rocha and R.O. Medrano, *Nonlinear Dyn.* **56** (2009) 389.
18. E. Campos-Cantón and I. Campos Cantón, *Rev. Mex. Fís.* **54** (2008) 411.
19. J.M. Muñoz-Pacheco and E. Tlelo-Cuautle, *Electronic Design Automation of Multi-Scroll Chaos Generators* (Bentham Sciences Publishers Ltd, 2010).
20. K.N. Salama, S. Özoguz, and A.S. Elwakil, *Proc. Int. Symp. on Circuits and Systems (ISCAS'2003)* **3** (2003) 176.
21. R. Senani and S.S. Gupta, *Electronic Lett.* **34** (1998) 829.
22. E. Tlelo-Cuautle, A. Gaona-Hernández, and J. García-Delgado, *Analog Integr. Circuits Signal Process.* **48** (2006) 159.
23. C. Sánchez-López, R. Trejo-Guerra and E. Tlelo-Cuautle, *Proc. 7th ICCDCS, ICCDCS* (2008) Cancun, México, ID-33.
24. R. Trejo-Guerra, E. Tlelo-Cuautle, C. Cruz-Hernández, and C. Sánchez-López, *Int. J. Bifurc. Chaos* **19** (2009) 4217.
25. C. Sánchez-López, R. Trejo-Guerra, J.M. Muñoz-Pacheco, and E. Tlelo-Cuautle, *Nonlinear Dynam* (2010), doi: 10.1007/s11071-009-9652-3
26. T. Tsubone and T. Saito, *IEEE Trans Circ Sys I* **45** (1998) 172.
27. M. Storace and F. Bizzarri, *IEEE Trans Circ Sys I* **54** (2007) 620.
28. Data Sheet AD844: www.analog.com/en/other/militaryaerospace/ad844/products/product.html
29. M. Parodi, M. Storace, and P. Julián, *I J Circ Theory Apps* **33** (2005) 307.
30. C. Wen and X. Ma, *IEEE Trans Circ Sys I* **55** (2008) 1328.
31. M. Delgado-Restituto, J. Ceballos-Cáceres, and A. Rodríguez-Vázquez, *Proc. IEEE Int Symp Circuits and Systems* (1996) 469.
32. M. Kachare, J. Ramírez-Angulo, R. Gonzalez Carvajal, and A.J. López-Martín, *IEEE Trans Circ Sys I* **52** (2005) 2033.
33. M.S. Bhat, S. Rekha, and H.S. Jamadagni, *19th Int Conf on VLSI Design* (2006), doi:10.1109/VLSID.2006.88.
34. L.O. Chua, Kang, and Sung Mo, *Proceedings of the IEEE* **65** (1977) 915.
35. R. Trejo-Guerra, E. Tlelo-Cuautle, J.M. Muñoz-Pacheco, C. Cruz-Hernández, and C. Sánchez-López, Operating Characteristics of Mosfets in Chaotic Oscillators, in *Transistors: Types, Materials and Applications* (Nova Publishers, 2010).
36. J. Lu, G. Yang, H. Oh, and A.C.J. Luo, *Chaos, Solitons Fractals* **23** (2005) 1879.
37. L. Dieci, *J. Dynam. Differ. Equat.* **14** (2002) 697.
38. K. Ramasubramanian and M.S. Sriram, *Phys. Nonlinear Phenom.* **139** (2000) 72.
39. T.S. Parker and L.O. Chua, *Practical Numerical Algorithms for Chaotic Systems* (Springer-Verlag, NY, 1989).
40. G.H. Golub and C.V. Loan, *Matrix Computations*, 3rd ed. (The Johns Hopkins University Press, 1996).